Cohesive energy of 3*d* transition metals: Density functional theory atomic and bulk calculations

P. H. T. Philipsen and E. J. Baerends
Theoretical Chemistry Department, Vrije Universiteit, De Boelelaan 1083, 1081 HV Amsterdam, The Netherlands
(Received 26 October 1995; revised manuscript received 18 April 1996)

We report generalized gradient approximation (GGA) cohesive energies for 3*d* metals. The problem of obtaining atomic reference energies in density-functional theory is considered. The effect of going to nonspherical atomic charge distributions is much larger at the GGA than at the local-density approximation (LDA) level, but allowing fractional occupations of 3*d* and 4*s* shells has negligible effect. When nonsphericity effects are taken into account in the atomic reference energies, the average absolute error of 0.3 eV in the GGA cohesive energies is much smaller than the LDA error of 1.3 eV. The working of the GGA is analyzed in terms of the cohesive energy density and the charge inhomogeneity division of the exchange energy. The low-gradient limit in the GGA functionals is not important as regions with charge inhomogeneity $s<0.2$ have negligible contributions. [S0163-1829(96)10531-2]

I. INTRODUCTION

The cohesive energies of the third-row elements Sc-Zn are a severe test for any method to solve—approximately—the Schrödinger equation. The delocalized conduction electrons as well as the tight *d* states in the bulk crystals have to be described accurately. It should be emphasized that, at the same time, accurate energies are required for the free atoms, which may have a highly open shell character (in the beginning and middle of the transition series) or have almost (Cu) or completely (Zn) closed shells. This clearly is a formidable task for approximate density functionals for the energy, and one wonders if the currently popular model exchange-correlation (XC) energy densities, which depend on the local density and its gradient only, can achieve sufficient accuracy. However, the result of this paper is that the energy difference can be reasonably described by functionals of the GGA type,[1–3] without resorting to any empirical corrections.

Density-functional theory (DFT) has progressed beyond the level of a qualitative method since the introduction of the gradient corrections to the local-density approximation (LDA). Perdew and co-workers have shown[4] that the GGA affords atomization energies of seven hydrocarbon molecules with an accuracy of 3 kcal/mol. Calculations on the larger Gaussian-1 (G1) database[5,6] that consist of 55 molecules reveal similarly that the GGA predicts atomization energies that deviate on the average only 3.7 kcal/mol (Refs. 7 and 8) from experiment, quite independent of whether or not the nonlocal correction to the correlation is included, as long as the exchange is being gradient corrected. The molecules in the G1 database, however, do not contain transition metal complexes, where correlation is known to be of utmost importance, as the error of the Hartree-Fock approximation is large for such systems.[9] In this respect it is noteworthy that also first bond dissociation energies in transition-metal carbonyl complexes are being reasonably described by the GGA's, as has been reviewed in Ref. 10. Not surprisingly, the relative simplicity of the method gives rise to limitations, as is exemplified by the increasing overestimation of bond energies for cationic first-row transition-metal hydrides as one goes to the right in the periodic system.[11] Nonetheless, it is now widely accepted that the GGA's are, in the molecular case, an improvement over the LDA and in general afford bond energies of nearly chemical accuracy.[10] It is now becoming apparent that the GGA is able to describe larger parts of the potential-energy surface and can be a useful tool to calculate reaction barriers. Whereas the LDA quite often severely underestimates activation energies the GGA tends to reduce this underestimation,[12–15] and a recent study on activation energies of several elementary processes with formaldehyde has shown that the GGA can compete with the best *ab initio* calculations that are feasable for such a system.

With the encouragement provided by this promising development it is becoming increasingly fashionable to utilize gradient-corrected functionals for extended systems as well. Recent GGA results for molecule-surface interactions show dramatic improvement upon the LDA, repairing the threefold overbinding of the LDA in the case of CO on a Cu surface,[16] and similarly reducing the interaction energy of CO with Pd.[17] As in the molecular case the improvement does not seem to be limited to just the chemisorption energies but apparently holds for a wider domain on the potential-energy surface, since the GGA's correctly predict a barrier for dissociation of molecular hydrogen over the Cu(100) surface,[18–20] whereas the LDA predicts barrierless dissociation. The GGA's seem to afford a semiquantitative description also for metal (slab) -molecule interactions, although many more calculations should be carried out to investigate this further.

Also, in bulk calculations GGA's reduce the overbinding of the LDA, and for a fairly large number of *sp*-bonded solids the accuracy achieved is typically 0.3 eV.[21–23] For transition metals the situation is not so clear. The GGA's predict the correct antiferromagnetic fcc ground state for Mn at room temperature[24] and the ferromagnetic bcc structure for iron.[25,26] The cohesive energy of Fe is better than the LDA outcome but nevertheless far too large; according to Ref. 25 the error is 2.0 eV with the 1986 functional of Perdew and Wang (PW86, Refs. 2 and 27) and according to Ref. 26 it is 1.4 eV with the 1991 functional of Perdew and Wang (PW, Refs. 3 and 4). Körling and Häglund[28] have reported improved cohesive energies for all first-row transition met-

als, albeit with unsatisfactory large error bars, up to 0.8 eV. The uncertainty of Ref. 28 resides in the ground-state energy of the free atom that was estimated by adding an experimental correction[29] to the calculated energy of the atom in different spherical configurations, i.e., $d^{n-2}s^2$ or $d^{n-1}s$, the correction being the difference of the statistical multiplet average of that configuration and the ground-state energy. However, it has been pointed out by Ziegler *et al.*[30] that the the average-of-configuration energy cannot be calculated in this way since the exchange hole of this energy expression does not satisfy certain requirements on which the justification of the LDA and GGA approximations are based. They therefore advocate the exclusive use of energies from densities corresponding to single determinants. Most atomic and molecular multiplet energies may be obtained in this way, although the method is not without drawbacks. Strictly speaking, the multiplet procedure of Ref. 30 requires orbitals that transform according to the irreducible representations of the point group of the system (usually referred to as symmetry and equivalence restrictions). For atoms this implies the use of central-field orbitals. However, it is sometimes possible to lower the energy considerably by lifting these restrictions, and a possible strategy to determine the ground-state energy would be a search for the lowest energy over all self-consistently optimized determinantal (Kohn-Sham) states without any constraint (cf. Ref. 31). This procedure is adopted in this paper.

In this work we focus mainly on two GGA's. The first, BP, employs the 1988 exchange expression of Becke[1] and the 1986 correlation correction of Perdew.[2] The Becke exchange form produces the correct energy density in the asymptotic tail of any finite atomic or molecular system, and at the same time leads to a correct lowest-order gradient correction, only with a coefficient that is too large. The other functional, PW, has been introduced by Perdew and coworkers in 1991,[3] the exchange part of which has been modeled closely to the Becke form. Care has been taken, however, that it has the right coefficient in the low gradient limit, since correct low-gradient behavior is expected to play a vital role in the description of solids.[32]

The two exchange functionals mentioned thus far produce excellent atomic exchange energies, but do not equally improve the corresponding potential.[33,34] One would like to avoid the situation that a different GGA would have to be used in the calculation of local properties than in the calculation of integral properties. Therefore we will briefly discuss the Engel-Vosko (EV) exchange functional,[32] which was intended to lead to a more balanced quality improvement of both energy and potential. This functional, without a nonlocal correlation correction, improves the band structure of the transition-metal oxides FeO and CoO, but predicts lattice parameters that are far too large.[35] We combine the EV exchange with the PW correlation, and examine the ability of the resulting functional to predict energy differences.

II. METHODOLOGICAL DETAILS

Carrying out self-consistent field (SCF) calculations on atoms without the central-field constraint introduces the technical problem of difficult convergence. The reason is simply the near degeneracy of the orbitals belonging to sets that would be strictly degenerate in spherical symmetry (in particular the 3d orbitals in the transition metals). Extensive searching has been performed, using progressively lower point group symmetries, to identify the lowest energy obtainable. In Table I the energies are reported for all atoms in C_{4v} symmetry, with a specification of the lowest-energy electronic configuration in that symmetry. Going to lower point group symmetry yields insignificant further lowering of the energy. For instance, in the case of Co we find a solution in C_{3v} symmetry that is only 0.02 eV lower than the lowest state in C_{4v} symmetry. For other atoms with an experimental F ground state, i.e., Ti, V, and Ni this effect is even smaller.

For the atomic corrections we have lifted as much as possible symmetry restrictions on the density, but we have limited ourselves to integer occupation numbers per irreducible representation. If, as has been pointed out by Averill and Painter,[36] a SCF solution does not satisfy the aufbau principle, the energy can be lowered by allowing for fractional electron transfer from the highest occupied orbital to the one or more lower-lying unoccupied states up to the point where they become degenerate. Starting from the optimal occupations from Table I, we have determined the most optimal charge transfer for all nonaufbau atoms, the result of which can be found in Table II.

As pointed out before, another approach to calculate degenerate ground states is the multiplet method due to Ziegler *et al.*[30] that is applicable straightforwardly by identifying for all ground states of the transition-metal atoms a determinant that is a pure state function. Since according to Hund's rules the lowest-energy term of a configuration is the term with maximum L selected from all terms of maximum spin multiplicity, one can always find a Slater determinant, constructed from central-field orbitals, that corresponds uniquely to the lowest-energy term, namely, the one with maximum M_L and M_S. The corresponding densities have $D_{\infty h}$ symmetry, and the energies thus obtained will in general be higher than the result of the global minimization method, which does not restrict densities to $D_{\infty h}$ symmetry. In the case of Fe the difference between the methods is as large as 0.4 eV when calculated with a GGA (the effect is particularly large with GGA's that favor charge inhomogeneity more than the LDA does). This difference underlines the problem of present day approximate energy functionals, that the energy is not a constant on the domain of densities that correspond to a certain degenerate ground state. Consider the example of the degenerate p electron as in boron; the p_+ and the p_- orbitals generate a density that is invariant under rotations with respect to the z axis. With a superposition of the p_+ and the p_- orbital the p_x orbital can be constructed that has a density lacking this property, and the calculated energy will in general not be equal to that for the p_+ and p_- orbital densities. We note that the same degeneracy problem already exists if there is no spatial but only spin degeneracy, since the spin unrestricted density functionals are not invariant under rotation in spin space.

III. COMPUTATIONAL DETAILS

The free-atom calculations have been performed with the molecular Amsterdam density functional (ADF) program.[37–40] The orbitals up to 2p were kept frozen and a

TABLE I. Energy lowering (El in eV) when going from a spherically-symmetric spin-restricted reference configuration to C_{4v} and spherical spin unrestricted configurations.

		C_{4v} (spin polarized)				Spherical (spin polarized)			
El	ref. config.	occupations[a]	LDA	BP	PW	config.	LDA	BP	PW
Sc	d^1s^2	1100 1000	0.22	0.47	0.46		0.16	0.18	0.17
Ti	d^2s^2	1102 0000	1.18	1.58	1.61	d^3s^1	1.02	1.14	1.16
V	d^3s^2	1112 0000	2.87	3.23	3.26	d^4s^1	2.93	3.13	3.15
Cr	d^5s^1		spherical				5.12	5.47	5.46
Mn	d^5s^2	2112 1000	5.29	5.63	5.57		5.30	5.61	5.54
Fe	d^6s^2	2112 1100	3.87	4.41	4.36		3.54	3.74	3.70
Co	d^7s^2	2112 0102	2.96	3.52	3.51	d^8s^1	2.79	2.84	2.86
Ni	d^8s^2	2112 0112	2.43	2.71	2.72	d^9s^1	2.52	2.53	2.56
Cu	$d^{10}s^1$		spherical				0.20	0.26	0.24
Zn	$d^{10}s^2$		spherical				no correction		

[a]The occupations of the $4s$ and $3d$ electrons specifying the C_{4v} determinantal state that gives the lowest energy are described by two rows, one for eac spin, each row containing the occupations for A_1 ($3d_{z^2}$ and $4s$), B_1 ($3d_{x^2-y^2}$), B_2 ($3d_{xy}$), and E ($3d_{xz}$,$3d_{yz}$) symmetry respectively. Occupation 2 means that either two consecutive spin orbitals are occupied (A_1), or two degenerated spin orbitals (E).

triple-zeta Slater basis set was used with three $4p$ and three $4f$ polarization functions. We have repeated all these calculations with the ADF-BAND program, which can include numerical atomic orbitals (NAO's) in the basis, and calculates the energy with respect to the numerical spherical atom. It appeared to be necessary to add a $4d$ Slater-type orbital (STO) to the single $3d$ NAO in the Ni basis for a reliable estimate of the energy difference between the spherical Ni atom in the experimental configuration and the calculated ground state. This is due to the fact that the $3d$ NAO is calculated for the experimental d^8s^2 configuration, but the GGA's predict a d^9s^1 ground-state configuration. The basis set flexibility provided by the additional $4d$ STO is required to describe the more diffuse $3d$ AO in the configuration with higher d count. Finally both technically different methods agreed within 0.05 eV on the contents of Table I.

TABLE II. The extra energy gained (eV) by allowing for fractional occupation numbers in spherical and C_{4v} symmetry. These numbers can be added to the atomic corrections of Table I. Entries smaller than 0.01 eV are left out of the table. The fractionally occupied states in spherical symmetry are Ti, $4s\downarrow 3d\uparrow$; Fe and Co, $4s\downarrow 3d\downarrow$. In C_{4v} symmetry the fractionally occupied states are V, $A_1\uparrow B_2\downarrow$, Co, $A_1\downarrow E_1\downarrow$; and Ni, $A_1\downarrow B_1\downarrow$.

	C_{4v}			spherical		
El	LDA	BP	PW	LDA	BP	PW
Ti				0.01	0.01	0.01
V	0.09					
Fe				0.17	0.12	0.14
Co	0.01			0.02	0.02	0.01
Ni	0.15		0.01			

The bulk calculations were performed at the experimental geometry, as the energy gained by optimizing the lattice constant or crystal structure is fairly small for $3d$ metals,[25,42] and the PW functional predicts lattice constants very well in the transition-metal series.[43] The experimental crystal structure of Mn is fairly complicated and for this element we have taken the geometry from Ref. 28. We have used the first-principles linear combination of atomic orbitals program ADF-BAND (Ref. 44) with a basis set of the double-zeta +NAO–type for the $3d$ and $4s$ orbitals, replacing one Slater of the triple-zeta STO basis set by a numerical orbital. The $3s$ and $3p$ orbitals were represented by a single NAO. Tests on Ni showed no effect of addition of $3s$ and $3p$ STO's to the basis. As polarization functions we used two $4p$ and one $4f$ STO. Since we use a *quadratic* tetrahedron method[41] for the k-space integration, we are able to attain high accuracy while keeping the number of k points within reasonable limits. To test the convergence with respect to the integration in k space, we have done all calculations with two different accuracy settings for integration over the Brillouin zone. The grid according to the more accurate setting gave rise to more than two times as many symmetry-unique points as the less accurate setting. In case of an fcc lattice the sparser of the grids consisted of 65 points and the more dense one of 175 symmetry-unique points. The effect of more than doubling the k-space sampling on the cohesive energy never exceeded the 0.05 eV. Given the fairly large basis set and the high values for the parameters that control the accuracy of the integration in both real and reciprocal space, we estimate the

precision of the energies to be at least 0.1 eV.

In most calculations, we have employed LDA densities, with the parametrization of Vosko and co-workers[45] of the calculated[46] correlation energy of the electron gas. Also, for the PW functional we have used this parametrization, instead of their own proposal, to ensure that the differences between the functionals are not influenced by the way of parametrizing the homogeneous electron gas result. Explicit spin-unrestricted calculations were done for the ferromagnetic crystals Fe, Co, and Ni, and for the single atoms. Only for the optimization of the fractional occupation numbers for the GGA, see Table II, we have done fully self-consistent calculations, and hence used GGA densities instead of LDA densities. This was required as the energy minimum only truly coincides with the point where the fractionally occupied orbitals become degenerate if the calculations are fully self-consistent.

For the analysis of the GGA's in Sec. V we split up the exchange-correlation energy into contributions from different regions in space, and this involves the integration of step-like integrands. As Gauss-Legendre quadrature, which is employed throughout the integration scheme,[39,40] requires N points to integrate a polynomial of the order $2N-1$, many points are needed, since a step function is not easily approximated by a polynomial. We have solved this problem by, on one hand, limiting the number of subintervals, and on the other hand, increasing the number of points until an accuracy of 10% was reached for Figs. 3 and 5 in Sec. V.

IV. RESULTS

In Table I we have listed the optimized energies of the free atoms, in both C_{4v} and spherical symmetry, with respect to the spherical spin-restricted atom in the experimental ground-state configuration. In spherical symmetry the energy lowering is primarily due to spin polarization, although in some cases there is also a change of configuration (in Ti, V, Co, and Ni the configuration changes from $d^n s^2$ to $d^{n-1}s^1$). The spin-polarization energy can be several eV, and of course is largest (ca. 5.5 eV) for Cr with six parallel spins. When the symmetry is lowered to C_{4v} the largest effects occur for Fe and Co where the effect of going to a nonspherical charge distribution is as much as 0.7 eV for the GGA's. Our result for Fe agrees reasonably well with the 0.8 eV that we infer from Ref. 47 for the PW functional. Unfortunately Ref. 47 does not specify the determinantal wave function, so the cause of this small discrepancy remains unknown. In general the LDA shows much smaller nonsphericity effects than the GGA's. This is in agreement with the general notion, as explained clearly by Perdew and co-workers,[4] that the exchange correction of the GGA favors densities that have on the average a high value of the dimensionless expansion parameter $s=(24\pi^2)^{-1/3}|\nabla\rho|/\rho^{4/3}$ that describes the inhomogeneity of the system, an effect which is only partly opposed by the nonlocal correlation correction. Stated somewhat more loosely: GGA's favor less smooth densities more than the LDA does. This can be seen immediately from the GGA expression for the exchange energy,

$$E_x^{\mathrm{GGA}}[\rho]=-C_X\int \rho^{4/3}F(s)d\mathbf{r}, \qquad (1)$$

where the enhancement factor $F(s)$ starts at 1 when the density gradient and therefore s is zero and increases with increasing inhomogeneity s, thus leading to a more negative exchange energy. The more stabilizing effect of GGA when the density gradients are larger also qualitatively explains that the GGA correctly predicts Fe to have a bcc lattice,[25] whereas the LDA predicts fcc, as one may expect a smoother density for the highly coordinated fcc atoms. The GGA also correctly predicts top site adsorption for CO on Cu (Ref. 16) whereas the LDA prefers the fourfold coordinated hollow site.

TABLE III. Absolute values of the cohesive energies (eV) of first-row transition metals, as calculated with the LDA, and the gradient corrected functionals BP and PW. The energies are with respect to the C_{4v} atoms of Table I.

El	LDA	BP	PW	exp.
Sc	4.87	3.84	4.11	3.90
Ti	6.29	4.87	5.09	4.85
V	6.49	4.90	5.12	5.31
Cr	5.22	3.58	3.80	4.10
Mn	5.19	3.44	3.73	2.92
Fe	6.25	4.52	4.78	4.28
Co	6.51	4.67	4.88	4.39
Ni	5.98	4.33	4.52	4.44
Cu	4.29	3.12	3.30	3.49
Zn	1.91	0.98	1.17	1.35

The effects of lifting the restriction of integer occupation numbers are summarized in Table II. In spherical symmetry a significant lowering $\sim$0.1 eV of the energy is obtained for the iron atom, and in C_{4v} symmetry a similar amount is gained by the LDA for the V and Ni atoms. In the GGA, however, the nonspherical atoms profit not more than 0.01 eV from the extra freedom: for the GGA the lifting of the symmetry restriction has a much larger impact than allowing noninteger occupations.

In Table III and in Fig. 1, the cohesive energy is presented for the LDA and the two GGA's. We see that the PW functional gives a slightly smaller correction to the LDA than BP, but both clearly improve very much upon the LDA, the average absolute error dropping from 1.3 eV in the LDA case to 0.3 eV for both GGA's. The large overbinding for iron reported by Refs. 25 and 26 can partly be ascribed to the unphysical spherical restriction on the density of the iron atom. The remaining discrepancy of 0.3 eV with the PW result of Ref. 26 can be related to the approximate nature of the linear-muffin-tin-orbital–atomic-spheres approximation (LMTO-ASA) method that these authors used. The result of Ref. 25 is a bit puzzling, since if we calculate the BP86 result with a spherical reference atom we arrive at a cohesive energy that is 1.2 eV lower than that of Ref. 25. In the cases where the reference atoms are spherical (Cr, Cu, Zn) PW seems to outperform the BP functional.

The results of the EV functional, which are not included in the table, lead to an average absolute error of 1.1 eV, and the severe overbinding of the LDA is replaced by an almost equally severe underbinding. This is consistent with the prediction of lattice constants that are much too large for a variety of metals,[35] confirming the conclusion that this func-

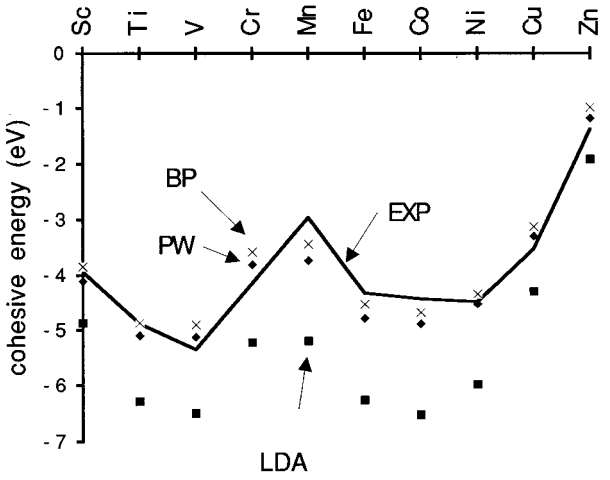

FIG. 1. Cohesive energies from Table III according to experiment, and as calculated with the functionals LDA, BP, and PW. The cohesive energies are defined here as $E(\text{crystal})-E(\text{atoms})$.

tional is unsatisfactory for energies, as well as for for the energy *difference* between atom and bulk.

The crucial quantity in DFT calculations for which approximations are required is the XC part of the energy. Our results suggest that the GGA approximation to this quantity is quite good as far as energy differences are concerned. It is interesting to analyze the influence of this energy term on the results. What can be expected for the XC contribution to the cohesive energy? Roughly speaking, the exchange energy becomes more negative with the number of spin-aligned valence electrons, and since usually there are more parallel spins in the atom than in the bulk, a repulsive exchange contribution may be expected that rises from Sc to Cr and drops for later transition metals. The correlation energy (also stabilizing) is roughly proportional to the number of electron pairs. As the valence electron pairing increases going from the atom to the bulk, correlation should increase the bonding energy, again with a maximum for Cr. In Fig. 2 it is seen that the GGA (PW) yields a repulsive exchange contribution to the cohesive energy, in accordance with the foregoing argument, except for the fringe elements Sc and Zn. The shape of the curve is also in agreement with our expectations. The

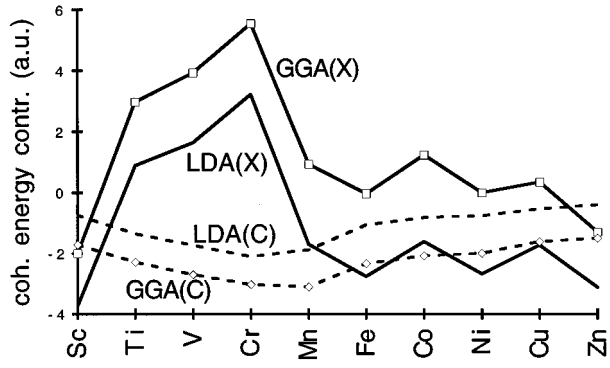

FIG. 2. Exchange (X) and correlation (C) contributions to the cohesive energy in both the LDA and (the BP form of) the GGA. (Positive contributions are *anti*bonding.)

LDA, however, predicts a bonding exchange contribution for Mn to Zn, a result that defies our expectations for the middle transition metals. Apparently, the well-known LDA underestimation of the exchange energy in atoms is not fully carried over to the bulk. It is clear that the GGA exchange curve resembles its LDA equivalent, but it is shifted upwards by ~ 2 eV. The bonding role of the exchange energy for Sc and Zn (also for the GGA) may be related to the atomic configuration: in Sc the interaction between the aligned $3d^{\uparrow}$ and $4s^{\uparrow}$ electrons is very weak since the $4s$ is much more diffuse than the $3d$, and in Zn the number of aligned electrons is the same for the atom as in the bulk. The loss of spin-polarization energy when going to the bulk will thus be small (or zero) and the argument given above for a repulsive exchange contribution to the cohesive energy does not apply. This, of course, does not explain the fact that, actually, there is a bonding contribution of the exchange energy for Sc and Zn.

With respect to the correlation energy we note that the expected bonding correlation contribution to the cohesive energy is reproduced by both the LDA and the GGA, as shown in Fig. 2. The GGA correlation curve is very much like the LDA result shifted downwards ~ 1 eV. Since the GGA results for both exchange and correlation exhibit approximately uniform shifts with respect to LDA through the transition-metal series, the GGA's do not effectively improve the trend of the cohesive energy through the series, cf. Fig. 1, although they do improve substantially the absolute values.

V. ANALYSIS OF THE GGA's

We will now study the effect of the GGA's on the bonding energy in more detail by first examining what regions in real space contribute to the XC energy. We will subsequently investigate the relative importance of regions where the density gradient is high (low), in order to better understand the differences between the BP and PW functionals. All data in this section refer to the Cu example.

In Fig. 3 we see how the XC part of the cohesive energy is built up in various spatial regions. For the construction of this figure we first note that the cohesive energy can be calculated as the integral over the unit cell of the energy density of the crystal minus the sum of the energy densities of the free atoms, located at the bulk positions, i.e., as a unit-cell integral over what could be called the cohesive energy density. To gain some insight into what regions are important for this integral, we divide the unit cell (the standard Wigner-Seitz cell) in spherical shells around the Cu atom at the center of the cell. These spherical shells will eventually be truncated by the unit-cell boundaries and only the part within the unit cell is taken into account. The largest distance from Cu to the unit-cell boundary is 3.4 bohr. The total integral is split up into contributions from the different regions constructed in this way. In the figure we show the contributions of a few XC energy terms to what is conceptually the spherically integrated cohesive energy density. A point at r stands for the contribution of the spherical shell surrounding r with thickness $\Delta r = 0.34$. First we see that the LDA exchange and correlation curves have a similar shape, starting with a repulsive part in the atomic region followed by an attractive part

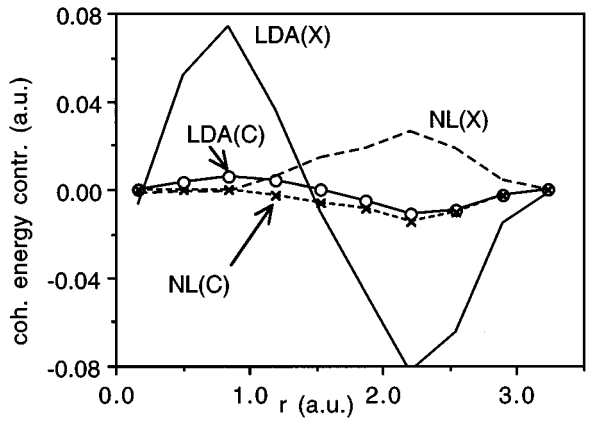

FIG. 3. Contributions from spherical shells, see text, to some cohesive energy terms for Cu: LDA exchange, LDA correlation, and the NL part of the exchange and correlation of the BP functional. The bond midpoint is at 2.4 a.u., the largest distance from the cell center to the boundary is 3.4 bohr. A point at r stands for the integral over a shell with thickness $\Delta r = 0.34 a_0$.

in the bond region. In view of the proportionality to ρ (the LDA exchange energy density is for instance simply $-C_X \rho^{4/3}$), this must reflect a charge flow from the atomic to the bonding region. The gradient corrections (representing the change from LDA to GGA) are close to zero in the atomic region, but in the bonding region (the bond midpoint is at 2.4 bohr) there is a repulsive gradient correction to the exchange, compensated partly by an attractive correlation correction. It is interesting to observe that the curves of the gradient corrections for exchange and for correlation resemble each other, the correlation correction having an opposite sign and being smaller in magnitude than the exchange correction. The gradient corrections in the figure pertain to the BP functional, but the result is virtually indistinguishable in the case where the PW functional was used. It is to be noted that the gradient corrections come from the bonding region, a result that may be understood as follows (cf. the analysis of Ref. 48). The gradient corrections depend, apart from the magnitude of the density and the volume considered (in this case spherical shells with volume proportional to r^2), on the inhomogeneity parameter s ($s=(24\pi^2)^{-1/3}|\nabla\rho|/\rho^{4/3}$), which is relatively small in the atomic region, but increases exponentially in the outer region of atoms where the density decays exponentially. In the bonding region we are dealing with points that fall in the outer regions of the constituting atoms, with concomitant high s's, but in the crystal the density gradients are very low around the bond midplane (often exactly zero at the bond midpoint by symmetry). The gradient corrections will thus in the bonding region be much larger for the atomic energy densities than for the crystal energy density. The positive sign (repulsive character) of the exchange correction and the negative sign of the correlation correction follow immediately from the stabilizing (destabilizing) nature of the exchange (correlation) gradient corrections.

The difference between the functionals BP and PW is mainly due to the exchange expression. For Cu the difference in cohesive energy is for 0.2 eV due to exchange and only for 0.03 eV due to correlation. In the expression for the

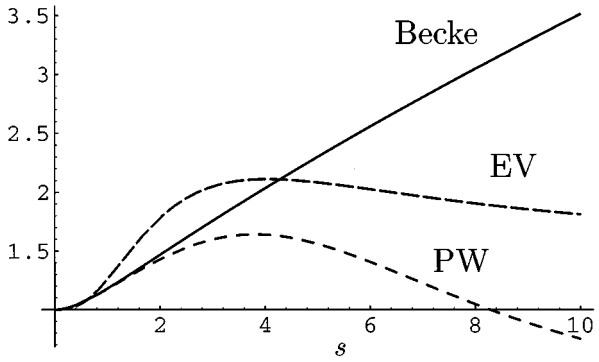

FIG. 4. Enhancement factor $F(s)$ [see Eq. (1)] of the exchange energy for the gradient-corrected functionals under study.

exchange energy, Eq. (1), an enhancement factor $F(s)$ appears which is plotted in Fig. 4 for the three exchange functionals of Becke88, EngelVosko93, and PerdewWang91, the $F=1$ case leading to the LDA result. Since $F^B > F^{\mathrm{PW}}$ for all s, the Becke functional always gives a more negative exchange energy than PW: $E_x^B < E_x^{\mathrm{PW}}$. We also have $F^B \geqslant 1$ and consequently $E_x^B < E_x^{\mathrm{LDA}}$. For very large inhomogeneities $s>8$, F^{PW} becomes smaller than one, going asymptotically to zero, which could lead to a less negative exchange energy than the LDA. However this is not the case, even in atoms where s diverges in the tails one finds $E_x^B < E_x^{\mathrm{PW}} < E_x^{\mathrm{LDA}}$.[49] The PW functional was constructed in such a way that it reverts for small s to the gradient expansion approximation (GEA) form $F^{\mathrm{GEA}}(s) = 1 + c_2 s^2$, with $c_2 = 0.1234$ a.u. The Becke functional has a gradient coefficient c_2 that is 2.2 times too large. The deviation of F^{PW} from F^B due to this low gradient limit is only significant for $s<0.2$.[32] The Becke exchange functional[1] was tailored such that it creates the exact asymptotic energy density for an electron far away from the molecule, by choosing a specific large-s form for F. Clearly PW spoils this exact long-range behavior, as it goes to zero to satisfy nonuniform scaling relations. So we have one functional with the correct low gradient limit and another describing the atomic tails better. Which part of the correction factor is important for the gradient correction to the exchange energy? To answer this question we write the nonlocal (NL, i.e., gradient-correction) part of the GGA exchange as an integral over s:

$$E_x^{\mathrm{NL}} = \int W(s)(F(s)-1)\,ds, \tag{2}$$

with the weight function $W(s)$ being the integral of the LDA exchange energy density over the subvolume where the density has the inhomogeneity s. To get an impression of the integrand in Eq. (2), we split the integral up into different ranges of s. (We note that a similar analysis for atoms has recently been made by Zupan *et al.*[50]) The ranges are chosen logarithmically between $s=0.1$ and $s=8$, the contributions from other s being negligible in our example (Cu crystal). In Fig. 5 the integral over an s region is given by a point in the center of that region and these points add up to the total integral. In Fig. 5(a) we see that the weight function $W(s)$ has an extremum for $s \sim 0.5$, in both the atomic and the bulk

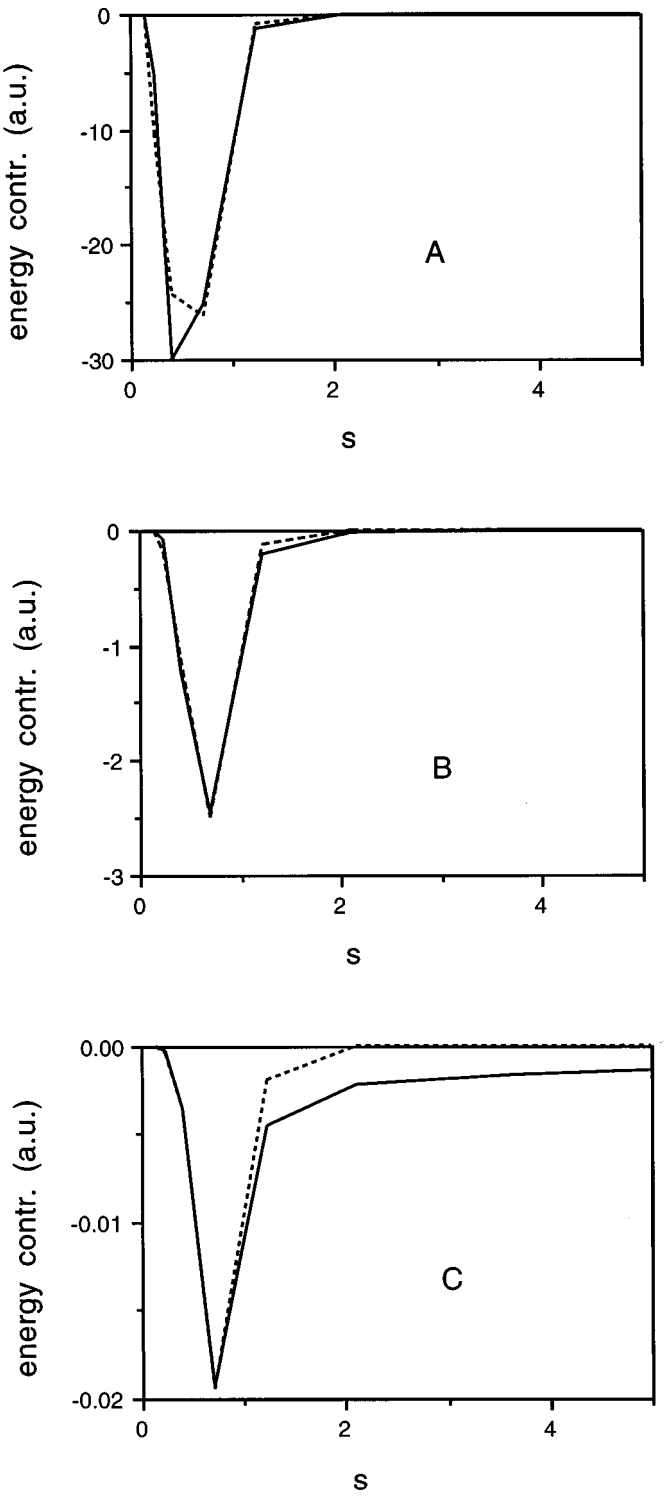

FIG. 5. Subdivision of the exchange energy according to charge inhomogeneity s, see Eq. (2), in the Cu atomic (drawn line) and bulk case (broken line). The exchange energy can be written as an integral over s and data points in this set of figures represent the integral over such a range and hence give an impression of the integrand itself. The ranges are chosen logarithmically as is explained in the text. (a) Weight factor $W(s)$ of Eq. (2) that is the s distribution of the LDA exchange energy. (b) $W(s)[F^{\mathrm{PW}}(s)-1]$, the s distribution of the nonlocal PW correction to the exchange energy. (c) $W(s)[F^{B}(s)-F^{\mathrm{PW}}(s)]$, the s distribution of the difference between the BP and PW exchange energies.

case. Although in the atoms high values of s occur in the atomic tails, the value of $W(s)$ is negligible for $s>2.5$ since there is negligible charge with such a high gradient. Figure 5(b) shows the splitting up, according to density inhomogeneity, of the PW exchange correction for the atomic and the bulk calculation. The important conclusion is that the low gradient region $s<0.2$ does not contribute to the nonlocal correction at all: even in the bulk the total contribution from $s<0.2$ is less than 0.02 eV per atom. This is a combined effect of the small value of $W(s)$ (there is not much charge with such a small gradient) and the small deviation of $F(s)$ from one in that region. In Fig. 5(c) the difference between the Becke and PW exchange functional is plotted, and since $F^{B}>F^{\mathrm{PW}}$ the result is always negative. The difference in the bulk between the two functionals comes almost entirely from the $s<1$ region. Both exchange functionals lower the bulk total energy, B more than PW, but the difference is determined by the value of F at intermediate s values. In the atomic calculation the Becke exchange energy density is also more negative at higher s values. So the result that Becke gives smaller cohesive energies than PW comes from the fact that Becke gets more energy lowering out of the atomic tails. It now is also understandable that the EV exchange correction is much larger, since F^{EV} has a steeper slope in the important $s\sim 1$ region, thus favoring nonsmooth densities more than the other functionals.

VI. SUMMARY

In conclusion, we have shown that the GGA's BP and PW are clearly an improvement over the LDA for predicting cohesive energies of first-row transition metals. This result is only obtained if the lowest-energy determinantal state for the atoms, without symmetry restrictions, is used to obtain the atomic reference energy. The effect of symmetry lowering is large as the GGA's are sensitive to density gradients and therefore to the choice of atomic reference determinant. The restriction to integer occupation numbers proves to have negligible influence on the GGA atomic energies. The overbinding of the LDA appears to be related to a not sufficiently repulsive exchange contribution to the cohesive energy (even negative, i.e., bonding for elements to the right of Cr). The GGA demonstrates, much more in line with qualitative expectations, a repulsive role of the exchange energy in the formation of these metals except Sc and Zn. Analysis of the XC contribution to the cohesive energy density shows that the repulsive nonlocal corrections to the cohesive energy originate from the bonding region. In contrast, the LDA exchange-correlation cohesive energy density is bonding in the bonding region and derives its overall repulsive character from a significant antibonding contribution from the atomic region. The splitting up of the exchange energy integral into subvolumes with a certain charge inhomogeneity s reveals that the GGA exchange energy is very sensitive to the value of the enhancement factor $F(s)$ for s somewhat smaller than one, whereas the precise form of $F(s)$ for other s is not as important. Therefore the fact that the PW functional has a correct low gradient limit is not important for its performance. The result that the EV nonlocal correction for the

exchange energy is much larger than the BP and PW nonlocal corrections is due to the large slope of the enhancement factor of this (EV) functional for $s \sim 1$. The performance of the EV functional on cohesive energies is very poor as the severe LDA overbinding is replaced by an almost equally severe underbinding.

ACKNOWLEDGMENTS

This work was supported by the Netherlands Foundation for Chemical Research (SON), with financial aid from the Netherlands Organization for Scientific Research (NWO). Extensive use was made of the supercomputing facilities of the National Computing Facilities Foundation (NCF).

[1] A. D. Becke, Phys. Rev. A **38**, 3098 (1988).
[2] J. P. Perdew, Phys. Rev. B **33**, 8822 (1986).
[3] J. P. Perdew, *Electronic Structure of Solids '91*, edited by P. Ziesche and H. Eschrig (Akademie Verlag, Berlin, 1991).
[4] J. P. Perdew, J. A. Chevary, S. H. Vosko, K. A. Jackson, M. R. Pederson, D. J. Singh, and C. Fiolhais, Phys. Rev. B **46**, 6671 (1992).
[5] J. A. Pople, M. Head-Gordon, D. J. Fox, K. Raghavachari, and L. A. Curtiss, J. Chem. Phys. **90**, 5622 (1989).
[6] L. A. Curtiss, C. Jones, G. W. Trucks, K. Raghavachari, and J. A. Pople, J. Chem. Phys. **93**, 2537 (1990).
[7] A. D. Becke, J. Chem. Phys. **96**, 2155 (1992).
[8] A. D. Becke, J. Chem. Phys. **97**, 9173 (1992).
[9] M. A. Buijse and E. J. Baerends, J. Chem. Phys. **93**, 4129 (1990).
[10] T. Ziegler, Chem. Rev. **91**, 651 (1991).
[11] T. Ziegler and J. Li, Can. J. Chem. **72**, 783 (1994).
[12] L. Fan and T. Ziegler, J. Am. Chem. Soc. **114**, 10 890 (1992).
[13] D. Porezag and M. R. Pederson, J. Chem. Phys. **102**, 9345 (1995).
[14] M. R. Pederson, Chem. Phys. Lett. **230**, 54 (1994).
[15] J. Baker, M. Muir, and Jan Andzelm, J. Chem. Phys. **102**, 2063 (1995).
[16] P. H. T. Philipsen, G. te Velde, and E. J. Baerends, Chem. Phys. Lett. **226**, 583 (1994).
[17] P. Hu, D. A. King, S. Crampin, M.-H. Lee, and M. C. Payne, Chem. Phys. Lett. **230**, 501 (1994).
[18] G. Wiesenekker, G. J. Kroes, and E. J. Baerends, J. Chem. Phys. **102**, 3873 (1995).
[19] B. Hammer, M. Scheffler, K. W. Jacobsen, and J. K. Nørskov, Phys. Rev. Lett. **73**, 1400 (1994).
[20] A. White, D. M. Bird, M. C. Payne, and I. Stich, Phys. Rev. Lett. **73**, 1404 (1994).
[21] M. Causà and A. Zupan, Chem. Phys. Lett. **220**, 145 (1994).
[22] Y. M. Juan and E. Kaxiras, Phys. Rev. B **48**, 14 944 (1993).
[23] Y. M. Juan, E. Kaxiras, and R. G. Gordon, Phys. Rev. B **51**, 9521 (1995).
[24] T. Asada and K. Terakura, Phys. Rev. B **47**, 15 992 (1993).
[25] T. C. Leung, C. T. Chan, and B. N. Harmon, Phys. Rev. B **44**, 2923 (1991).
[26] C. Amador, W. R. L. Lambrecht, and B. Segall, Phys. Rev. B **46**, 1870 (1992).
[27] J. P. Perdew and Y. Wang, Phys. Rev. B **33**, 8800 (1986).
[28] M. Körling and J. Häglund, Phys. Rev. B **45**, 13 293 (1992).
[29] R. E. Watson, G. W. Fernando, M. Weinert, Y. J. Wang, and J. W. Davenport, Phys. Rev. B **43**, 1455 (1991).
[30] T. Ziegler, A. Rauk, and E. J. Baerends, Theoret. Chim. Acta **43**, 261 (1977).
[31] F. W. Kutzler and G. S. Painter, Phys. Rev. Lett. **59**, 1285 (1987).
[32] E. Engel and S. H. Vosko, Phys. Rev. B **47**, 13 164 (1993).
[33] E. Engel and S. H. Vosko, Phys. Rev. B **47**, 2800 (1993).
[34] R. van Leeuwen and E. J. Baerends, Phys. Rev. A **49**, 2421 (1994).
[35] P. Dufek, P. Blaha, and K. Schwarz, Phys. Rev. B **50**, 7279 (1994).
[36] F. W. Averill and G. S. Painter, Phys. Rev. B **46**, 2498 (1992).
[37] E. J. Baerends, D. E. Ellis, and P. Ros, Chem. Phys. **2**, 42 (1973).
[38] E. J. Baerends and P. Ros, Int. J. Quantum Chem. Symp. **12**, 169 (1978).
[39] P. M. Boerrigter, G. te Velde, and E. J. Baerends, Int. J. Quantum Chem. **33**, 87 (1988).
[40] G. te Velde and E. J. Baerends, J. Comp. Phys. **99**, 84 (1992).
[41] G. Wiesenekker and E. J. Baerends, J. Phys. Condens. Matter **3**, 6721 (1991).
[42] A. T. Paxton, M. Methfessel, and H. M. Polatoglou, Phys. Rev. B **41**, 8127 (1990).
[43] V. Ozoliņš and M. Körling, Phys. Rev. B **48**, 18 304 (1993).
[44] G. te Velde and E. J. Baerends, Phys. Rev. B **44**, 7888 (1991).
[45] S. H. Vosko, L. Wilk, and M. Nusair, Can. J. Phys. **58**, 1200 (1980).
[46] D. M. Ceperley and B. J. Alder, Phys. Rev. Lett. **45**, 566 (1980).
[47] M. Castro and D. R. Salahub, Phys. Rev. B **49**, 11 842 (1994).
[48] R. van Leeuwen and E. J. Baerends, Int. J. Quantum Chem. **52**, 711 (1994).
[49] T. Zhu, C. Lee, and W. Yang, J. Chem. Phys. **98**, 4814 (1993).
[50] A. Zupan, J. P. Perdew, K.Burke, and M. Causà, Int. J. Quantum Chem. (to be published).